DETECTION OF STIMULI CHANGES IN NEURAL EVENTOGRAMS USING THE LINE OF SYNCHRONIZATION OF GLOBAL RECURRENCE PLOTS

G. Tzagkarakis[1]   *G. Palagina*[2]   *I. Smirnakis*[1]   *S. M. Smirnakis*[2]   *M. Papadopouli*[1,3]

[1] Foundation for Research and Technology-Hellas, Institute of Computer Science, Heraklion, Greece
[2] Brigham and Women's Hospital, Harvard Medical School, Boston, MA
[3] University of Crete, Department of Computer Science, Heraklion, Greece

ABSTRACT

Reliable detection of stimulus-driven states and their separation from internal state-driven spontaneous activity is an important step towards inferring temporal dynamics of neurons and its relation to the perception of external inputs. This is challenging, especially when no prior assumptions about the underlying model and data generating processes exist. To address this task, we applied efficient recurrence quantification analysis (RQA) based on global recurrence plots (RP) for accurate identification of the onset and offset of visual neuronal responses caused by distinct types of visual stimuli. In particular, these critical times are estimated by taking the first order difference of the line of synchronization extracted from the associated global RP. Our approach was evaluated using a real dataset of visually-driven neuronal responses and spontaneous activity (recorded by in vivo 2-photon calcium imaging). It accurately detects both the onset and offset time instants in the eventograms of pyramidal neurons in a completely model agnostic framework.

Index Terms— Recurrence quantification analysis, global recurrence plot, line of synchronization, neural eventograms, stimuli change detection

1. INTRODUCTION

A fundamental question in neuroscience is to understand how the sensory information is transformed and processed in the neocortex and subcortical structures to achieve optimal sensory perception of the environment. Neocortex, a six-layered, folded, sheet-like structure, consists of billions of interconnected neurons. Visual information is transferred from the retina via the lateral geniculate nucleus (LGN) to the primary visual cortex (area V1) and higher visual and association cortical areas. Neurons in area V1 fire action potentials when visual stimuli appear within their receptive fields, responding vigorously to visual stimuli that are close to their preferred orientation and direction. During visual exploration the information about the environment is encoded in real time via population firing patters appearing across multiple neurons. These patterns are highly variable due to ongoing spontaneous firing in the network, yet the perceptual outcomes are fairly faithful, even under degraded viewing conditions, such as low contrast. To build a good understanding of the contribution that ongoing activity and stimulus feature-related activity make to the perceptual outcome under varying viewing conditions, it is important to classify the states of the individual cells and their populations into stimulus-driven and ongoing spontaneous

activity-driven. We take advantage of recent improvements in massive population imaging via in vivo 2-photon microscopy, powerful non-linear data analysis techniques and the unique position of V1 in the mouse as an area that is both required for perceptual outcomes and has a large population of cells with simple, easy to track functional properties (such as orientation and direction-selectivity).

A critical question is how well is one able to use statistical features of the ongoing neuronal firing to identify "significant" firing events, that, for example, mark the detection of relevant stimulus in the environment or signify the occurrence of certain internal states. Despite the significant progress, the automatic detection of the stimulus-driven and spontaneous firing events, as well as detection of dynamic changes between distinct stimuli types, is an open problem.

The underlying dynamical system that governs the behavior of a neuron can be very complex, whilst its dynamical features are only partially observed through the corresponding "eventograms". Furthermore, the relevant physiological phenomena are typically a fusion of deterministic, chaotic, and random processes, yielding changes at multiple time scales, thus imposing significant challenges on the subsequent signal analysis.

Recurrence plots (RPs) [1] were proposed as an advanced graphical technique of visual nonlinear data analysis, which reveals all the times of recurrences, that is, when the phase space trajectory of the dynamical system visits roughly the same area in the phase space. Due to the highly subjective nature of a visual interpretation of RPs, *recurrence quantification analysis* (RQA) [2] was introduced to perform nonlinear analysis of time series, which is also able to treat nonstationary and short data series. RQA comprises of a set of appropriate quantitative measures for the quantification of recurrence structures, and the detection of critical transitions in the system's dynamics (e.g. deterministic, stochastic), which is precisely the objective of this work.

More specifically, our proposed methodology first computes a *global* RP for a given eventogram associated with a pyramidal neuron by appropriately embedding the one-dimensional eventogram into a higher-dimensional phase space. Then, the onset and offset instants between the distinct stimuli are detected by calculating the *line of synchronization* (LOS) from the global RP. This approach is motivated by our expectation that different stimuli will be characterized by different dynamics that can be distinguished by the RQA. Notice that, for now, we only focus on the detection of changes between stimuli, without taking into consideration their type. Overall, the contribution of this paper is a computationally-tractable method for an accurate detection of onset-offset instants of distinct stimuli from the associated neural eventogram. The proposed method is *generic, model-free, and totally agnostic* of the underlying dynamical system

that generates the neural signals.

The rest of the paper is organized as follows: Section 2 refers to the differences between our proposed methodology and prior studies. Section 3 analyzes the data acquisition process, whereas Section 4 describes in detail our proposed approach for detecting stimuli changes from the global RP of eventograms. Finally, Section 5 evaluates the performance of the proposed method on a real OGB-1 dataset, while Section 6 summarizes the main remarks and gives directions for further extensions.

2. RELATION TO PRIOR WORK

The method presented here takes advantage of the recurrence features in the form of a LOS, which is calculated directly from the given eventogram by exploiting its global RP, for the accurate detection of stimuli switching instants. The work in [3] calculates a thresholded RP from a sequence of interspike intervals, which is then coupled with a shuffling procedure that swaps neighboring intervals, in order to perform only a qualitative study about the predictability of spike trains. While the present study is related to recent works in how spike train firing patterns from a neuron represent external stimuli [4, 5, 6, 7, 8, 9, 10], our methodology capitalizes on a model-free, data agnostic perspective, which was not considered in these earlier studies. Specifically, several of the previous works are based on the assumption that spike trains are stationary processes (i.e., the stochastic properties of the neurons do not change in time), while their accuracy depends on the underlying mechanism that produces the spiking activity. Furthermore, some of these studies employ a Bayesian framework to model a spike train as a stochastic point process and the associated biological signal as a stochastic process based on its known properties. Despite its theoretical appeal, the performance of the Bayesian approach degrades dramatically when the assumed probability model is not a reasonable approximation to the data.

3. DATA ACQUISITION PROCESS

This section describes our data collection and pre-processing process. More specifically, we used male C57BL/6 mice expressing Td-Tomato in 65% of cortical Dlx5/6-positive interneurons. Total data set consists of 21 FOVs from 18 animals (aged 8-35 days). A craniotomy was placed over V1 and calcium-sensitive dye OGB-1 was bulk-injected to follow the population activity of V1 neurons via two-photon imaging [11]. For imaging we used a Prairie Ultima-IV two-photon microscope fed by a Chameleon Ti:sapphire Ultra-II laser. We imaged cells $120 - 200$ microns below the pia, in layer 2/3 of mouse V1, at 820 nm wavelength. Astrocytes (stained by red dye SR-101) were excluded from the analysis. We selected an FOV containing 100320 cells and acquired images using a 20x objective lens (0.95 NA) at 3.2 - 11 Hz. Total length of the spontaneous activity movies was 10-28 min.

Visual stimulation was performed in 4 adult animals. We used drifting square-wave gratings with a temporal frequency of 2 Hz and a spatial frequency of 0.05 cycles/^{o}, constructed with MATLAB psychophysics toolbox. Each visual presentation trial consisted of 2 sec of visual stimulus presentation, followed by 3 sec of spatially uniform illumination. Gratings (12 directions, 15-30 trials per direction) were shown in random sequence on a flat LCD monitor covering $60^o \times 80^o$ of the contralateral monocular visual field. See [12] for the in-detail description of data collection.

Cellular calcium data were expressed as dF/F and deconvolved using the method described in [13]. Per cell, the portion of the

recording containing no calcium events was used to estimate baseline noise. To produce an eventogram, inferred spikes overcoming the threshold of 2 standard deviations from baseline were set to 1, while the rest of the recording was set to zero. In the following, let $\mathbf{r} \in \mathbb{R}^N$ denote an eventogram, that is, the response of a given neuron, and $\mathbf{t} \in \mathbb{R}^N$ be the associated vector of indices (i.e., time instants) determining the time intervals when a specific stimulus occurs. Notice that $\mathbf{t}$ is a piecewise linear curve. Fig. 1 shows an eventogram selected at random from our OGB-1 dataset, along with the generating sequence of stimuli.
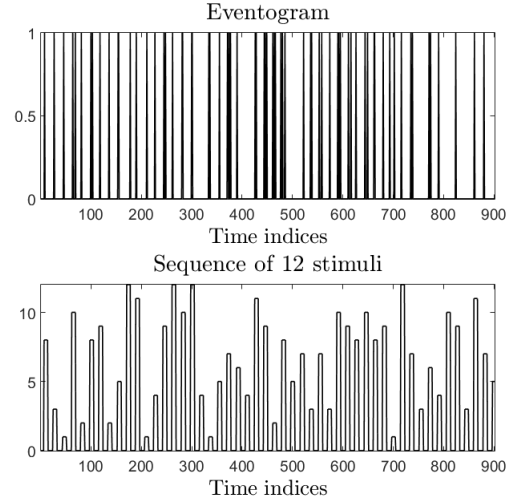

Fig. 1: Eventogram and corresponding sequence of stimuli.

4. DETECTION OF STIMULI CHANGES USING GLOBAL RECURRENCE PLOTS

This section describes in detail our proposed approach for detecting stimuli switching instants, by applying RQA on the global RP of the corresponding eventogram. We emphasize that, although the subsequent analysis is made for pyramidal neurons, however, the methodology is generic and applicable on any type of neurons.

4.1. Global recurrence plot of eventograms

First, we give a brief overview of the global RP, which is a key component of our proposed data analysis pipeline. More specifically, an RP is a square matrix whose elements correspond to those times at which a state of a dynamical system recurs, thus revealing all the times when the *phase space trajectory* of the dynamical system visits roughly the same area in the phase space. To this end, RPs enable the investigation of an m-dimensional phase space trajectory through a two-dimensional representation of its recurrences. Such recurrence of a state occurring at time i, at a different time j is represented within a two-dimensional square matrix with ones (recurrence) and zeros (non-recurrence), where both axes are time axes.

Given an eventogram of length N, $\{r_i\}_{i=1}^N$, a phase space trajectory can be reconstructed via time-delay embedding,

$$\mathbf{x}_i = [r_i, r_{i+\tau}, \ldots, r_{i+(m-1)\tau}], \quad i = 1, \ldots, N_s, \quad (1)$$

where m is the embedding dimension, τ is the delay, and $N_s = N - (m-1)\tau$ is the number of states. Having constructed a phase

space representation, an RP is defined as follows,

$$\mathbf{R}_{i,j} = \Theta\left(\varepsilon - \|\mathbf{x}_i - \mathbf{x}_j\|_p\right) , \quad i,j = 1, \ldots, N_s , \quad (2)$$

where $\mathbf{x}_i, \mathbf{x}_j \in \mathbb{R}^m$ are the states, ε is a threshold, $\|\cdot\|_p$ denotes a general ℓ_p norm (Euclidean distance ($p = 2$) is commonly used), and $\Theta(\cdot)$ is the Heaviside step function, whose discrete form is defined by

$$\Theta(n) = \begin{cases} 1, & \text{if } n \geq 0 \\ 0, & \text{if } n < 0 \end{cases} , \ n \in \mathbb{R} . \quad (3)$$

The resulting matrix $\mathbf{R}$ exhibits the main diagonal, $\mathbf{R}_{i,i} = 1$, $i = 1, \ldots, N$, also known as the *line of identity* (LOI). Typically, several linear (and/or curvilinear) structures appear in RPs, which give hints about the time evolution of the high-dimensional phase space trajectories. Besides, a major advantage of RPs is that they can also be applied to rather *short* and even *nonstationary* data.

A special case of RP, useful in studying phase space trajectories, is the *global* RP [14] (also called *unthresholded RP*). Instead of plotting the recurrences, the global version is simply obtained by plotting the distances between states $\mathbf{x}_i$ and $\mathbf{x}_j$, that is,

$$\mathbf{D}_{i,j} = \|\mathbf{x}_i - \mathbf{x}_j\|_p , \quad i,j = 1, \ldots, N . \quad (4)$$

The use of a global RP, $\mathbf{D}$, in our proposed approach is motivated by the fact that its thresholded counterpart, $\mathbf{R}$, can reveal convergence properties between the distinct time intervals within a given eventogram, $\mathbf{r}$, in the sense that the $\mathbf{R}_{i,j}$ values will indicate dynamics that occur to $\mathbf{r}$ within some critical distance. On the other hand, since we are interested in detecting precisely the onset and offset times between neighboring stimuli in the associated sequence $\mathbf{t}$, a global RP can enhance the understanding of the phase space trajectories and detect *phase synchronous* dynamics even when two distinct states of $\mathbf{r}$ do not converge.

Estimation of embedding parameters. In our implementation, the optimal time delay τ is estimated as the first minimum of the average mutual information (AMI) function [15]. Concerning the embedding dimension m, a minimal sufficient value is estimated using the method of false nearest neighbours (FNN) [16]. In practice, the minimal embedding dimension is defined as the dimension for which the fraction of false neighboring points is zero, or at least sufficiently small. Fig. 2 illustrates the optimal time delay and embedding dimension for the eventogram shown in Fig. 1.
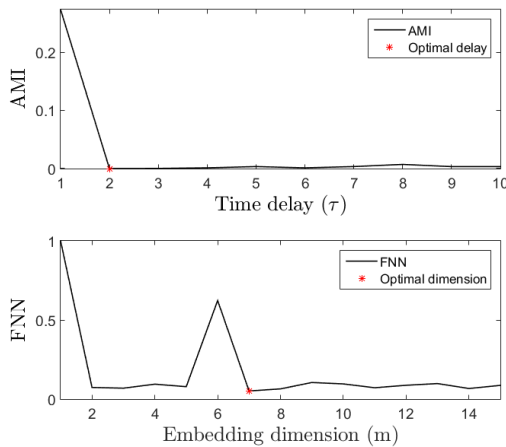

Fig. 2: AMI and FNN criteria for setting the embedding parameters of the eventogram in Fig. 1.

4.2. LOS-based stimuli onset/offset detector

A key property of RPs, which is exploited in the detection of stimuli switching instants, is that it reveals the local difference of the dynamical evolution of close trajectory segments in the phase space of an eventogram. A time dilation or a compression of the time intervals, where a stimuli appears in the eventogram, causes a distortion of the diagonal lines in the corresponding RP. Then, the LOI will be disrupted yielding the, so called, *line of synchronization* (LOS) [17]. Although the LOS is still continuous, it is not a straight diagonal line. This enables the estimation of a *non-parametric rescaling function* between the states of an eventogram.

Let $\mathbf{l} \in \mathbb{R}^{N_s}$ denote the LOS. The interpretation of $\mathbf{l}$ is the following: if $l_i = k$, for some $i = 1, \ldots, N_s$, then, the state of the eventogram at time i approximates the state at time k. In the case of eventograms, the LOS is a piecewise linear function, as shown in Fig. 3, which illustrates the global RP and the LOS (staircase line) for the eventogram shown in Fig. 1. Since, in general, $N_s \neq N$, in practice we apply a zero padding to $\mathbf{r}$ in order to obtain a LOS vector $\mathbf{l}$ whose length is equal to that of the index vector $\mathbf{t}$.

Finally, having estimated the LOS, we calculate the first order differences,

$$d_{l,i} = l_{i+1} - l_i , \ i = 2, \ldots, N . \quad (5)$$

Doing so, the vector $\mathbf{d}_l \in \mathbb{R}^N$ will be of the form,

$$\mathbf{d} = [\text{NaN}, \ldots, 0, d_i, 0, 0, \ldots, 0, d_j, 0, \ldots], \quad (6)$$

with the zeros corresponding to the intervals where the LOS is constant. Then, given that $d_i \neq 0$ and $d_j \neq 0$, we consider d_i to be the onset time and d_j the offset time of a stimulus. This interpretation is justified by the fact that the constant segments of the LOS, or equivalently the zero segments of $\mathbf{d}_l$, correspond to time periods in the eventogram whose dynamics, as expressed by the corresponding state vectors, are driven by the same stimulus.
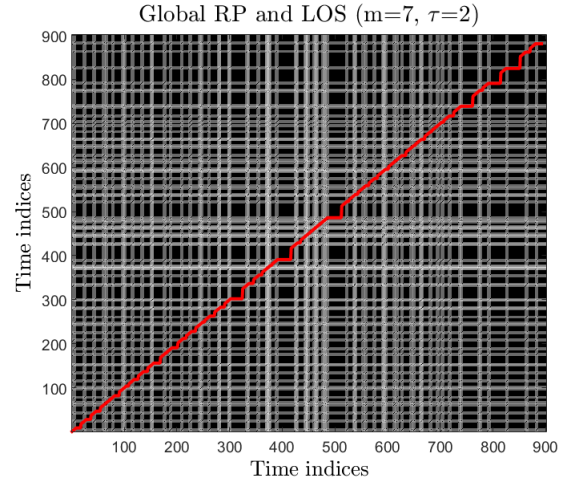

Fig. 3: Global RP and LOS for the eventogram in Fig. 1.

5. EXPERIMENTAL EVALUATION

The performance of our proposed methodology is evaluated on a set of real OGB-1 data, recorded as described in Section 3. In particular, a subset of the available dataset that includes all the eventograms with a firing rate exceeding 10 spikes/min is considered.

1271

This heuristic rule allows us to account for those eventograms that convey meaningful information for the associated sequence of stimuli. For each one of the 170 selected eventograms, the embedding parameters (m, τ) are estimated first using the AMI and FNN criteria, followed by the calculation of the corresponding global RP and the estimation of its LOS. All the computations involving the LOS have been performed using the CRP toolbox (http://tocsy.pik-potsdam.de/CRPtoolbox/).

The original and estimated onset and offset times for the eventogram (shown in Fig. 1) are depicted in Fig. 4. Clearly, the first order differences calculated from the LOS, which is extracted from the corresponding global RP, are capable of approximating accurately the onset/offset times between consecutive stimuli of different types. The achieved performance becomes even more significant given the completely model-agnostic framework and the lack of any prior assumptions about the data generating process or the probability distribution of the data.
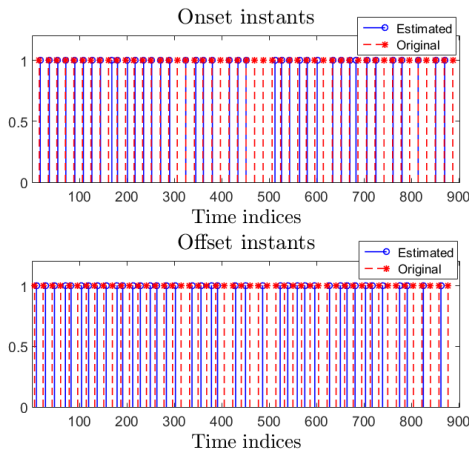

Fig. 4: Original and estimated onset/offset times for the eventogram in Fig. 1.

The estimation accuracy for the whole subset of the 170 eventograms is presented in Fig. 5, which shows the histograms of the differences between the original and estimated onset times (Fig. 5(a)), as well as between the original and estimated offset times (Fig. 5(b)). Positive differences mean that the original onset (respectively offset) times precede the estimated ones, while negative values correspond to the the cases when the estimated onset (respectively offset) times follow the original ones. In general, the greatest mass of the onset time differences is concentrated around 1, whilst the offset time differences vary mainly between 0 and 2 time instants, revealing in both cases the efficiency of the RQA-based method in estimating accurately the occurrence of each stimulus.

Note that the onset estimates are on average more accurate than the offset estimates. This likely has to do with the biological properties of cortical neurons, namely the spike-frequency adaptation. The adaptation properties (e.g. how fast the firing rates decline after initial burst on presentation of optimal stimulus) are highly variable between individual neurons, with most adapting neurons showing adaptation within 800 ms after stimulus onset [18]. Since our stimuli stay on for 2 seconds, this presents an ample opportunity for firing adaptation for many neurons, thus their event rates change insignificantly when the stimulus is turned off, as most of the decline has already occurred due to adaptation. The detection of offsets will likely improve when short stimuli (e.g 50-100 ms) are used.
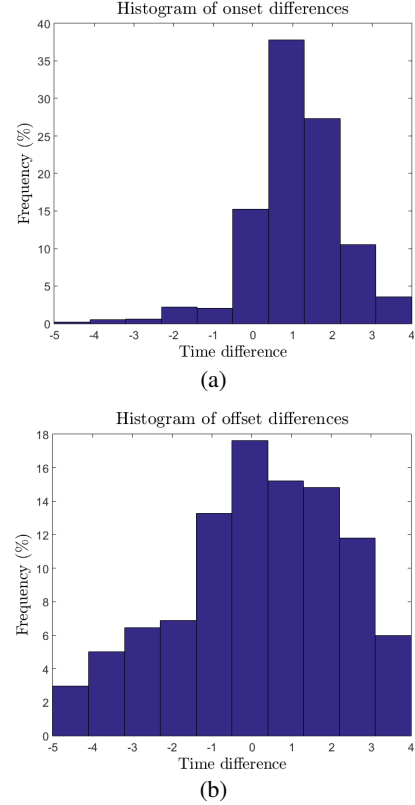

Fig. 5: Histograms of (a) onset time differences and (b) offset time differences, between the original times and the RQA-based estimates.

6. CONCLUSIONS AND FUTURE WORK

This work proposes a new methodology for the accurate estimation of onset/offset times between distinct stimuli, by exploiting the LOS extracted from the global RP of an eventogram, which is associated with the specific sequence of stimuli. Experimental results on a real OGB-1 dataset revealed the potentials of this approach, whose main advantage is its totally model-free framework and lack of dependence on prior knowledge about the underlying data distribution and stimulus.

Currently, the estimation process considers single cell eventograms. We expect that the performance will improve by also accounting for potential correlation between the eventograms, which will be reflected in their cross RP. The analysis of the population eventograms will take into account the interplay between individual neurons in the biological (functional) network and will enable us to identify and study the functionally-significant recurrent features of the population activity and their contribution to the encoding of external stimuli and internally-occurring states. We also plan to incorporate the type of stimulus and type of neuron (e.g., pyramidal vs. interneuron as well as its orientation preference) and assess their impact. Finally, the use of the Euclidean norm as a distance metric can be restrictive. To this end, we will study the performance of general ℓ_p norms, where the value of p will better adapt to the given data.

7. REFERENCES

[1] J.-P. Eckmann, S. Kamphorst, and D. Ruelle, "Recurrence plots of dynamical systems," *Europhysics Letters*, vol. 5, no. 9, pp. 973–977, Nov. 1987.

[2] J. Zbilut and C. Webber, "Embeddings and delays as derived from quantification of recurrence plots," *Physics Letters A*, vol. 171, no. 3–4, pp. 199–203, Dec. 1992.

[3] P. Kaluzni and R. Tarnecki, "Recurrence plots of neuronal spike trains," *Biological Cybernetics*, vol. 68, pp. 527–534, 1993.

[4] W. Bialek, F. Rieke, R. R. de Ruyter van Steveninck, and D. Warland, "Reading a neural code," *Science*, vol. 252, no. 5014, pp. 1854–1857, 1991.

[5] D. K. Warland, P. Reinagel, and M. Meister, "Decoding visual information from a population of retinal ganglion cells," *Journal of Neurophysiology*, vol. 78, no. 5, pp. 2336–2350, 1997.

[6] E. N. Brown, L. M. Frank, D. Tang, M. C. Quirk, and M. A. Wilson, "A statistical paradigm for neural spike train decoding applied to position prediction from ensemble firing patterns of rat hippocampal place cells," *Journal of Neuroscience*, vol. 18, no. 18, pp. 7411–7425, 1998.

[7] M. C. Wiener and B. J. Richmond, "Decoding spike trains instant by instant using order statistics and the mixture-of-poissons model," *Journal of Neuroscience*, vol. 23, no. 6, pp. 2394–2406, 2003.

[8] R.E. Kass, V. Ventura, and C. Cai, "Statistical smoothing of neuronal data," *Network: Comput. Neural Syst.*, vol. 14, pp. 5–15, 2003.

[9] A. E. Brockwell, A. L. Rojas, and R. E. Kass, "Recursive bayesian decoding of motor cortical signals by particle filtering," *Journal of Neurophysiology*, vol. 91, no. 4, pp. 1899–1907, 2004.

[10] Y. Hirata and K. Aihara, "Representing spike trains using constant sampling intervals," *Journal of Neuroscience Methods*, vol. 183, no. 2, pp. 277–286, 2009.

[11] C. Stosiek *et al.*, "In vivo two-photon calcium imaging of neuronal networks," *PNAS 100*, vol. 12, pp. 7319–7324, 2003.

[12] A. Palagina et al., "Inhibitory units: An organizing nidus for feature-selective sub-networks in area v1," *bioRxiv 282988*, 2018.

[13] J. T. Vogelstein *et al.*, "Fast nonnegative deconvolution for spike train inference from population calcium imaging," *Neurophysiol.*, vol. 104, no. 6, pp. 3691–704, Dec. 2010.

[14] J. Iwanski and E. Bradley, "Recurrence plots of experimental data: To embed or not to embed?," *Chaos*, vol. 8, no. 4, pp. 861, 1998.

[15] A. M. Fraser and H. L. Swinney, "Independent coordinates for strange attractors from mutual information," *Phys. Rev. A*, vol. 33, pp. 1134–1140, Feb. 1986.

[16] M. B. Kennel, R. Brown, and H. D. Abarbanel, "Determining embedding dimension for phase-space reconstruction using a geometrical construction," *Phys. Rev. A*, vol. 45, pp. 3403, 1992.

[17] N. Marwan, M. Thiel, and N. R. Nowaczyk, "Cross recurrence plot based synchronization of time series," *Nonlin. Processes Geophys.*, vol. 9, pp. 325, 2002.

[18] B. Ahmed *et al.*, "Estimates of the net excitatory currents evoked by visual stimulation of identified neurons in cat visual cortex," *Cerebral Cortex*, vol. 8, no. 5, pp. 462–476, 1998.